Activity Coefficient and Vacancy-Flow Effects on Diffusion in Silver-Gold Alloys*

R. O. MEYER† AND L. M. SLIFKIN
University of North Carolina, Chapel Hill, North Carolina
(Received 25 April 1966)

Ten measurements have been made of the mean atom drift for silver and gold tracer atoms placed at the interface of silver-gold alloy diffusion couples. A new technique for marking the original interface, using radioactive hafnium oxide, was developed. The existence of a broad minimum in the plot of D^* versus composition allowed a detailed investigation of the effects of a vacancy flux and activity-coefficient gradient on tracer diffusion, since a Kirkendall vacancy flux could be produced in a couple throughout which D^* was essentially constant. The largest contribution to the mean atom drift results from the gradient of activity coefficient. The effect of Kirkendall lattice distortion on the drift was calculated and was found to be comparable to the vacancy-flux effect. Good agreement was found between the experimental drift and the net calculated effect. The existence of an impedance to free diffusion across the welded interface of a diffusion couple was demonstrated. Measurements of tracer diffusion coefficients, interdiffusion coefficients, marker shifts, and void positions are also reported.

I. INTRODUCTION

THE detailed theoretical analysis of diffusion in a chemical-concentration gradient in binary alloys was begun by Darken[1] and LeClaire[2,3] and continued by Manning.[4–7] These analyses show that three distinct factors determine an atom's movement: its self-diffusion coefficient D_i^*, the activity coefficient γ_i, and the Kirkendall vacancy flow. The role of self-diffusion coefficients in diffusion has been extensively investigated in measurements on chemically homogeneous specimens and is therefore not of primary concern to the present work. The effect of the activity coefficient on diffusion, as described by Darken and LeClaire, has been generally substantiated by measurements of chemical interdiffusion coefficients, but such experiments are not very accurate compared to tracer experiments. The effects on the drift of these atoms of a net vacancy flow and of gradients of the diffusion coefficient and activity coefficient were investigated in an early experiment by Manning.[4] In this work, however, the contribution from the diffusion-coefficient gradient dominated the results and all other effects were often smaller than the experimental uncertainties.

An experiment, then, is needed in which the activity coefficient and vacancy-flow effects can be critically evaluated. Because of the manner in which the self-diffusion coefficients vary with composition, such an experiment is possible in the silver-gold system. It consists of the measurement of the average displacement of tracer atoms originally placed at the interface of a diffusion couple, in this respect similar to Manning's experiment. The mean atom drift depends on the self-diffusion coefficient through gradD^*. By choosing compositions such that gradD^* is nearly zero throughout the diffusion couple, this effect, usually dominant, is virtually eliminated. The variation of D^* for both silver and gold at 950°C is shown in Fig. 1, taken from the data of Mallard *et al.*[8] Using couples composed of 14 and 56 at.% gold, respectively, with gold tracer at the interface, and couples composed of 30 and 66 at.% gold, respectively, with silver at the interface, it is apparent that grad D^* is nearly zero. At the same time there will be a substantial Kirkendall flow, since D_{Ag}^* is always more than twice as large as D_{Au}^*.

Another advantage of the silver-gold system for this experiment is the existence of accurate thermodynamic data. Several sources[9–13] of data have been considered to be reliable in a critical analysis by White, Orr, and Hultgren.[14] The activity-coefficient effect on diffusion is conveniently expressed in terms of the factor $(1+\partial \ln\gamma/\partial \ln N)$. Values of this factor, calculated from these data, are shown in Fig. 2 for 950°C, and are believed to be good to approximately 4% over the composition range employed in this experiment.

The analysis that follows is applicable to any face-centered-cubic binary alloy, but will be written explicitly for silver-gold alloys. Based on the work of Huntington and Grone[15] and of Penney,[16] it is assumed for the large specimens used in the present work that

* Supported in part by the U. S. Atomic Energy Commission.
† National Science Foundation Predoctoral Fellow, 1964–65; present address: University of Arizona, Tucson, Arizona.
[1] L. S. Darken, Trans. AIME **174**, 184 (1948).
[2] A. D. LeClaire, Progr. Metal Phys. **1**, 306 (1949); **4**, 265 (1953).
[3] A. D. LeClaire, Phil. Mag. **3**, 921 (1958).
[4] J. R. Manning, Phys. Rev. **116**, 69 (1959).
[5] J. R. Manning, Phys. Rev. **124**, 470 (1961).
[6] J. R. Manning, Phys. Rev. **139**, A126 (1965).
[7] J. R. Manning (to be published).
[8] W. Mallard, A. Gardner, R. Bass, and L. Slifkin, Phys. Rev. **129**, 617 (1963).
[9] O. Kubaschewski and O. Huchler, Z. Elektrochem. **52**, 170 (1948).
[10] C. L. McCabe, H. M. Schadel, Jr., and C. E. Birchenall, J. Metals **5**, 709 (1953).
[11] R. A. Oriani, Acta Met. **4**, 15 (1956).
[12] C. Wagner and G. Engelhardt, Z. Physik. Chem. **159**, 241 (1932).
[13] A. A. Zhukovitzkii, S. N. Krynkov, M. E. Yanitskaya, and A. G. Golitsyn, Dokl. Akad. Nauk SSSR **102**, 121 (1955).
[14] J. White, R. Orr, and R. Hultgren, Acta Met. **5**, 747 (1957).
[15] H. B. Huntington and A. R. Grone, J. Phys. Chem. Solids **20**, 76 (1960).
[16] R. V. Penney, J. Phys. Chem. Solids **25**, 335 (1964).

lateral dimensional changes due to the action of the surface as a source and sink for vacancies are negligible. In addition, edge effects on tracer diffusion have been eliminated in the usual way, by removing material from the sides of the specimen. The problem, then, is reduced to one of one dimension.

II. THEORY

Tracer atoms placed at the interface of a diffusion couple with ends of different compositions will undergo a net average displacement due, firstly, to gradients in the self-diffusion coefficient and activity coefficient. Atoms in a diffusion-coefficient gradient will tend to move in the direction of increasing D^*, since they are more mobile in that direction. Atoms in an activity-coefficient gradient will tend to move in the direction of decreasing γ, where they are bound more strongly to their neighbors. In addition, the Kirkendall vacancy flow that exists in a chemical-concentration gradient affects the mean atom drift of tracers in two ways: (a) If the net vacancy flow is from right to left, a tracer atom will be approached more frequently from the right and will therefore have a tendency to move preferentially to the right; (b) since the net atom flow which accompanies the net vacancy flow is confined to the diffusion zone, the crystal will gain atomic planes on that side of the interface from which the vacancies are supplied and will shrink on the other side of the interface. A distinction will be made between these two Kirkendall-type effects, with the first denoted as the vacancy-flow effect and the second as the lattice-distortion effect.

In his early paper, Manning[4] extended the treatment of LeClaire[3] to obtain $\bar{x}$, the mean atom drift or shift of the center of gravity of the tracer profile relative to the interface marker. He obtained the result

$$\bar{x}=2\tau\int_{-\infty}^{+\infty} c_i^*D_i^*K(\partial N_i/\partial x)dx \Big/ \int_{-\infty}^{+\infty} c_i^*dx, \quad (1)$$

where τ is the diffusion time, c_i^* is the concentration of type-i tracer atoms, and N_i is the atom fraction (chemical) of type-i atoms in the alloy. The quantity K in Eq. (1) contains the details of the various contributions to the shift. In subsequent papers[5–7] Manning has recalculated the quantities in K, taking more carefully into account the correlations between successive atom and vacancy jumps. His most complete result for K is

$$K=\frac{\partial \ln D_i^*}{\partial N_i}-\frac{\partial \ln\gamma_i}{\partial N_i} \pm\frac{2(w_{Ag}-w_{Au})}{7.15W}\left(1+\frac{\partial \ln\gamma_i}{\partial \ln N_i}\right)f_{Au}f_{Ag}\alpha, \quad (2)$$

where w_i is the jump frequency of a type-i atom into an existing adjacent vacancy, $W=N_{Ag}w_{Ag}+N_{Au}w_{Au}$ is an average jump frequency, f_i is the correlation factor, and α is a function of the ratio D_{Ag}^*/D_{Au}^* and is nearly constant with the value of 1.27 for the present work. The plus sign is to be used for gold tracer while the minus sign is to be used for silver tracer.

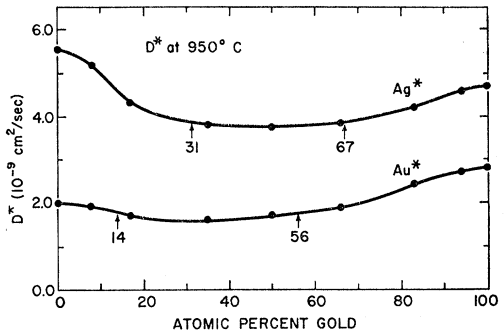

FIG. 1. Self-diffusion coefficients in the silver-gold system at 950°C.

The first two terms in Eq. (2) were originally obtained by LeClaire[3] and represent the contributions to the mean atom drift due to gradients in the self-diffusion coefficient and activity coefficient. When substituted for K in Eq. (1) they yield what will be denoted as $\bar{x}_{D^*,\gamma}$. The remainder of Eq. (2) represents the effect of a vacancy flow on the mean atom drift, but does not include the effect of lattice distortion. The result obtained when this last term is substituted in Eq. (1) will be denoted as $\bar{x}_{\text{vac flo}}$.

The contribution to the mean atom drift due to lattice distortion, denoted as $\bar{x}_{\text{latt dist}}$, was estimated by Manning to be about $\frac{1}{5}x_m$, where x_m is the calculated Kirkendall marker shift. This contribution can be calculated more exactly by noting that nondiffusing particles, or equivalently, lattice points, move within the diffusion zone because of the creation and annihilation of lattice planes. Darken's[1] velocity equation has been modified by Manning[7] to give

$$v(x,t)=-(D_{Ag}^*-D_{Au}^*)(1+[\partial \ln\gamma_i/\partial \ln N_i]) \times\alpha(\partial N_{Au}/\partial x), \quad (3)$$

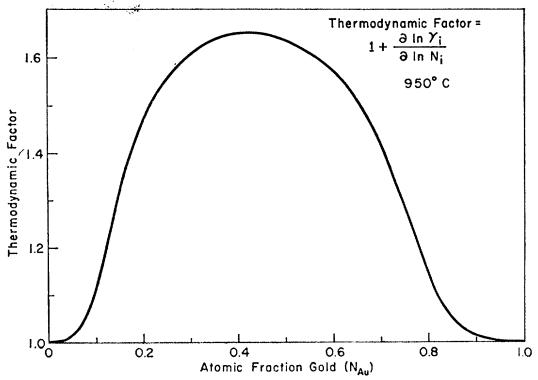

FIG. 2. The thermodynamic factor $(1+\partial \ln\gamma/\partial \ln N)$ for the silver-gold system at 950°C.

where α is the same factor that appears in Eq. (2). Hence, in addition to the tracer drift velocity resulting from a preference for jumping in one direction rather than the other, there will also be a drift velocity due to the motion of the lattice. Since the net drift is measured relative to the interface marker, the drift velocity which affects the measurement is the velocity relative to the interface marker:

$$v_R(x,t)=v(x,t)-v(x_0,t). \tag{4}$$

In Eq. (4), x_0 is the position of the interface marker, so that $v(x_0,t)$ is the interface-marker velocity.

The average net drift for tracer atoms due to lattice distortion is thus given by

$$\bar{x}_{\text{latt dist}}=\frac{\left(\int_{-\infty}^{+\infty}\int_0^{\tau} c_i^*(x,t)v_R(x,t)dxdt\right)}{\int_{-\infty}^{+\infty} c_i^*(x,\tau)dx}. \tag{5}$$

Since all of the experimental information will be known only for time τ, at the end of the diffusion anneal, the integration over t in Eq. (5) must be carried out. The tracer concentration c_i^* varies as $t^{-1/2}$ times a function of $(x/t)^{1/2}$ and the chemical composition N_i will be a function of $(x/t)^{1/2}$, so that the integrand can be written as

$$c_i^*(x,t)v_R(x,t)=t^{-1/2}g(\eta)\{\partial N_i/\partial x\}=t^{-1}f(\eta), \tag{6}$$

where η has been written for $(x/t)^{1/2}$. The numerator of Eq. (5) is then equivalent to the iterated integral $\int_0^{\tau} t^{-1/2}\{\int_{-\infty}^{+\infty} f(\eta)d\eta\}dt$. The order of integration can now be changed with the result

$$\bar{x}_{\text{latt dist}}=2\tau^{1/2}\int_{-\infty}^{+\infty} f(\eta)d\eta \Big/ \int_{-\infty}^{+\infty} c_i^*(x,\tau)dx$$

$$=2\tau\int_{-\infty}^{+\infty} c_i^*(x,\tau)v_R(x,\tau)dx \Big/ \int_{-\infty}^{+\infty} c_i^*(x,\tau)dx. \tag{7}$$

It may be noted that $v_R(x,t)$ has the same functional dependence on $(x/t)^{1/2}$ as do the other drift terms calculated by Manning, and that the method of integration given here yields the same result for these other terms [Eq. (1)] as obtained by Manning. (It appears, however, that Manning's method of integration[4] is not correct, although his result is correct.)

Equation (7) can be simplified further by inserting Eq. (4) for $v_R(x,\tau)$.

$$\bar{x}_{\text{latt dist}}=\left(2\tau\int_{-\infty}^{+\infty} c_i^*(x,\tau)v(x,\tau)dx \Big/ \int_{-\infty}^{+\infty} c_i^*(x,\tau)dx\right)$$

$$-2\tau v(x_0,\tau). \tag{8}$$

The second term in Eq. (8) is the familiar Kirkendall marker shift x_m with $v(x_0,\tau)$ calculated from Eq. (3). Inserting Eq. (3) into Eq. (8) yields the final expression for the lattice-distortion contribution in terms of convenient quantities:

$$\bar{x}_{\text{latt dist}}=\frac{-2\tau\int_{-\infty}^{+\infty} c_i^*(D_{\text{Ag}}^*-D_{\text{Au}}^*)[1+(\tau\,\ln\gamma_i/\partial\,\ln N_i)]\alpha(\partial N_{\text{Au}}/\partial x)dx}{\int_{-\infty}^{+\infty} c_i^*dx}+x_m, \tag{9}$$

where all quantities are evaluated at time $t=\tau$ and, as before, x_m is the calculated Kirkendall marker shift.

TABLE I. Description of alloy couples used.

Couple	Temp. (°C)	Diffusion time τ(sec) ($\times 10^4$)	Composition[a] end A (at.%Au)	Composition[a] end B (at.% Au)	Tracer applied to end A
1	950	8.43	14.2	56.3	Au^{198}
2	950	8.51	14.5	55.7	Au^{198}
3	950	8.43	55.7	14.0	Au^{198}
4	950	8.51	56.5	14.0	Au^{198}
5	950	4.27	30.5	30.5	Au^{198}
6	950	4.36	30.8	30.8	Au^{198}
7	950	1.96	30.4	66.4	Ag^{110}
8	950	1.96	66.4	30.4	Ag^{110}
9	950	1.90	30.0	66.3	Ag^{110}
10	950	1.90	66.3	30.0	Ag^{110}

[a] For couples Nos. 5 to 10, compositions which are listed as the same value represent neighboring faces of adiacent pieces of the same ingot.

III. EXPERIMENTAL PROCEDURE

Ten $\frac{3}{8}$-in.-diam cylindrical couples with a thin layer of radioactive Ag or Au tracer, together with a nondiffusing $Hf^{181}O_2$ marker placed in the interface, were diffused at approximately 950°C. The specimens making up the couples were either single crystals or bi- or tricrystals, vacuum-grown from 99.999% pure silver and 99.9% (or better) pure gold. End A of each couple was about $\frac{1}{2}$ in. long and was the end which would subsequently be held in the lathe chuck during sectioning. End B of the couple was about $\frac{1}{8}$ in. long and was prepared with accurately parallelled surfaces so that the exposed surface of end B could later serve as a reference plane for alignment in the sectioning lathe. Diffusion times τ (corrected to 950°C), compositions, and tracers used are summarized for each of the ten couples in Table I. Couples Nos. 1 to 4 and couples Nos. 7 to 10 satisfied the condition that grad D_i^* be nearly zero.

Couples No. 4 and No. 5 were chemically homogeneous and were designed to check the possible existence of any impedance to free diffusion across the welded interface. Since there were so few variations of the diffusion parameters (temperature, time, composition, tracer) among the ten runs, the data obtained thus afforded an excellent check on the reproducibility of the experiment and, as discussed below, allowed an evaluation of the quality of the interface weld.

The requirement of accuracy in the range of a few microns suggested several unusual experimental techniques. Details of these features are summarized below.

A. Surface Preparation

During the preparation of the cylindrical components of the couple, it was found that by mounting them in a ring of similar metal and molding this in a larger ring of dental acrylic (a plastic that dissolves in acetone), it was possible to polish surfaces very flat, as gauged by interference fringes. On couples Nos. 1 to 4 the runout was between $\frac{1}{2}$ and 2 μ, while on all other couples the surfaces were flat to $\frac{1}{4}$ μ or better.

After polishing, the specimens were annealed. Since the diffusion anneal was to be at the relatively high temperature of 950°C, where grain boundary diffusion would not be important, this preanneal had the primary function of eliminating work-hardening at the interface surfaces. Work-hardened surfaces would interfere with the welding process which was to follow. Couples Nos. 1 to 6 were annealed in a carbon boat which was continuously evacuated. This had the unfortunate effect of thermally etching away some material from the polished surfaces. Couples Nos. 7 to 10 were consequently annealed in small evacuated and sealed Vycor capsules and there was no appreciable evaporation loss. As a result of this change in procedure, the surfaces and hence the subsequent welding of couples Nos. 7 to 10 are believed to be better than for couples Nos. 1 to 6.

B. Couple Assembly

A radioactive tracer, either Au^{198} or Ag^{110}, was plated on end A of each couple. Instead of using small wire interface markers, radioactive $Hf^{181}O_2$ was deposited by precipitation onto the surface of end B of each couple. Such a nondiffusing radioactive marker has the advantage of allowing both distortion-free welds and a well-defined couple interface. $Hf^{181}O_2$ was chosen because it is readily available, does not diffuse, is quite refractory, and has a sufficiently long half-life. The γ radiation of Hf^{181} can be easily separated from that of Au^{198} or Ag^{110} with a radiation analyzer.

The couple components were welded in a spring-loaded device under a pressure of about 150 psi at approximately 875°C for about 45 min. This method yielded mechanically strong couples without producing objectionable distortion.

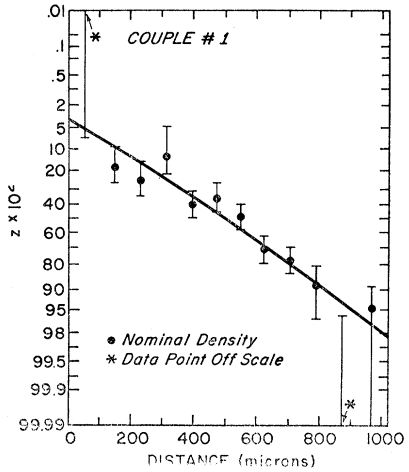

FIG. 3. Probability plot for couple No. 1.

It should be noted here that, for some of the couples, end A, on which the tracers were plated, was the gold-rich end, while for the remaining couples, end A was the silver-rich end. This was done in anticipation of the existence of a weld impedance, so that any effect on the measured tracer shift would increase the shift for some couples and decrease it for others. These two geometries are evident from Table I.

C. Diffusion Analysis

After a diffusion anneal, the couples were sectioned, and the γ activity and mass of each section were measured by standard techniques.[17] The density of silver-gold alloys varies appreciably with composition, so that it was necessary to determine the density of each section in order to obtain cut thicknesses from chip weights. Because of this large density change, how-

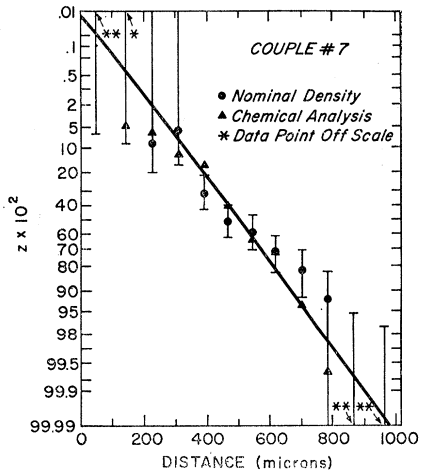

FIG. 4. Probability plot for couple No. 7.

[17] C. T. Tomizuka, in *Methods of Experimental Physics* (Academic Press Inc., New York, 1959), Vol. 6A, p. 364.

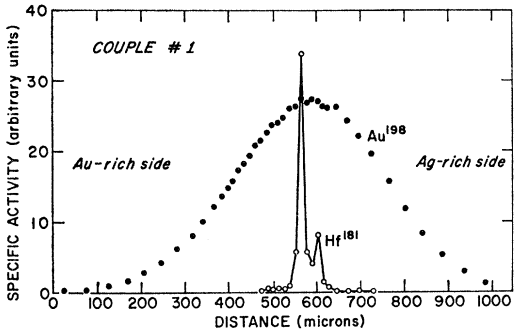

FIG. 5. Specific activity of Au^{198} and Hf^{181} in couple No. 1.

ever, the determination of density was equivalent to the determination of composition, so that once the densities were found, the compositions needed in the theoretical expressions were also determined.

The procedure for obtaining densities began with computation of the nominal density of a combination of several adjacent sections from their weights and from thickness determined by the lathe settings. Although the accuracy of the lathe settings was not very good, by taking several of the sections together, advantage was taken of the noncumulative nature of this error. Using the terminal-density values determined previously by careful bulk-density measurements, these combined-section nominal density values were plotted on arithmetic-probability paper. Examples of such data, along with appropriate error bars, are shown in Figs. 3 and 4. Next a smooth curve was drawn through these nominal density points. The slope of this curve at several composition points was determined from the relation

$$\tilde{D}=1/\{4\tau(\text{slope})^2\}. \qquad (10)$$

Here $\tilde{D}$ was calculated from Manning's[7] modification of the Darken equation:

$$\tilde{D}=(N_{\text{Au}}D_{\text{Ag}}^*+N_{\text{Ag}}D_{\text{Au}}^*)(1+[\partial \ln\gamma_i/\partial \ln N_i])S. \qquad (11)$$

The quantity S is a function of $D_{\text{Ag}}^*/D_{\text{Au}}^*$ and is nearly constant with the value of 1.04 for the present work. The use of Eq. (10) is discussed by Johnson[18] and is strictly applicable only to cases where $\tilde{D}$ is constant. Since $\tilde{D}$ over the composition range of the diffusion couples is not exactly constant (it varies by 30%), the use of Eq. (10) for determining slopes of the density curve is only approximate. These smooth curves are also shown in Figs. 3 and 4.

As a check on the accuracy of the procedure just described, a wet chemical analysis was performed on couples Nos. 4 and 7 to 10. Although the absolute accuracy of this analysis was only about 3 at.% Au, the precision within a set of analyses was about $\frac{1}{2}$ at.% Au. The results of each set of analyses were therefore all adjusted by a proportional factor so that the terminal compositions agreed with values known quite accurately from previous bulk-density measurements. These chemical values are also shown in Fig. 4.

[18] W. A. Johnson, Trans. AIME 147, 331 (1942).

TABLE II. Experimentally and theoretically obtained mean atom drifts.[a]

Couple	$\bar{x}_{D^*,\gamma}$ (μ)	$\bar{x}_{\text{vac flo}}$ (μ)	$\bar{x}_{\text{latt dist}}$ (μ)	$\bar{x}_{\text{theor}}$ (μ)	$\bar{x}_{\text{expt}}$ (μ)
1	+28	−4	−8	+16	+15
2	···	···	···	+··	+17
3	···	···	···	−··	−5
4	−26	+5	+9	−12	+2
5	0	0	0	0	+7
6	0	0	0	0	+6
7	−14	−4	−5	−23	−26
8	···	···	···	···	+34
9	···	···	···	···	−27
10	+14	+3	+5	+22	+34

[a] The sign convention used throughout the experiment gives a plus sign to a shift toward end A, and a minus sign to a shift toward end B. By consulting Table I, it can be seen that the theoretical shifts are toward the silver-rich end for couples Nos. 1—4 and toward the gold-rich end for couples Nos. 7—10. It should be noticed that the experimental shift for couple No. 4 is in the wrong direction, presumably because of a poor weld.

With specific activities calculated utilizing values given by the smooth probability curve, all that remained was to determine the interface position. The interface position was taken at the center of a section if the Hf^{181} activity was all contained in that section. When the Hf^{181} activity was contained in two sections, its position was taken proportionately between the two sections. The Hf^{181} was apparently distributed over about half a section thickness, probably due to misalignment in sectioning, so that by locating its activity peak in the manner described, the accuracy was roughly a quarter of the section thickness (or about ± 4 μ), rather than half a section thickness.

IV. RESULTS

Specific activities of radioactive tracers and markers are shown as a function of distance in Figs. 5–7 for couples Nos. 1, 5, and 7. Shifting the distance coordinate x so that $x=0$ coincided with the marker position, the mean atom drift was obtained from

$$\bar{x}_{\text{expt}}=\int_{-\infty}^{+\infty} c_i^* x dx \Big/ \int_{-\infty}^{+\infty} c_i^* dx, \qquad (12)$$

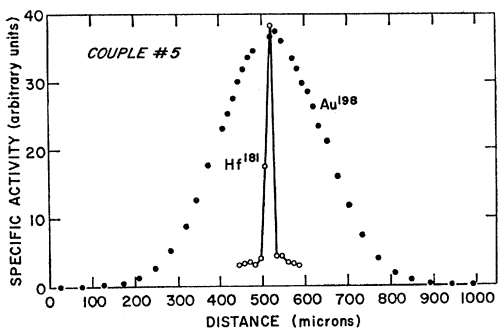

FIG. 6. Specific activity of Au^{198} and Hf^{181} in couple No. 5.

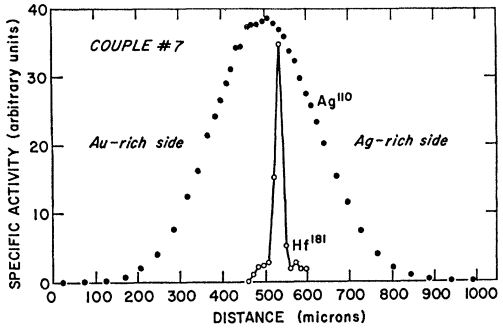

FIG. 7. Specific activity of Ag^{110} and Hf^{181} in couple No. 7.

where c_i^* is the tracer specific activity. Equation (12) was integrated graphically by taking the area under the polygon formed by connecting all data points with straight lines. A correction was applied to the denominator to account for the finite extent of the data. No correction was necessary for the numerator. The experimental results $\bar{x}_{\text{expt}}$ are shown in Table II. The error in $\bar{x}_{\text{expt}}$ is approximately $\pm 4\mu$ and is primarily due to uncertainty in location of the interface marker.

Theoretically predicted results were calculated from Eqs. (1), (2), and (9) by a similar graphical integration. Values for N_i and $\partial N_i/\partial x$ were obtained from the smooth curves on the probability plots. Experimental values of specific activity were used for c_i^*. Diffusion and activity coefficients D_i^* and γ_i were obtained as functions of N_i from the literature sources mentioned earlier. Correlation factors f_i and jump frequencies w_i were found by solving simultaneously the following two equations:

$$f_i = 3.58W/(w_i + 3.58W), \tag{13}$$

$$D_{\text{Au}}^*/D_{\text{Ag}}^* = f_{\text{Au}}w_{\text{Au}}/f_{\text{Ag}}w_{\text{Ag}}. \tag{14}$$

Equation (13) is a modification by Manning[19] of the LeClaire-Lidiard[20] equation.

The predicted values of the several contributions to $\bar{x}$ and also their sum, $\bar{x}_{\text{theor}}$, are shown in Table II. The errors resulting from uncertainties in the quantities appearing in the equations and from graphical procedures are estimated to be $\pm 10\%$ for the silver tracer and about $\pm 20\%$ for the gold tracer. It should be noted that $\bar{x}_{D^*,\gamma}$ is almost entirely due to the activity coefficient term. Because of the almost constant D_i^* values and the symmetry of D_i^* versus N_{Au} about the minimum, the diffusion-coefficient gradient only contributes about 15% of $\bar{x}_{D^*,\gamma}$.

V. DISCUSSION

Couples Nos. 1 to 4 all have essentially the same diffusion parameters, so they should all yield the same result. The same statement is true of couples Nos. 7 to 10. It is seen from Table II that experimental results are not the same, but that they fall into two sets of agreeing values, with the exception of couple No. 4, for which the measured shift was in the wrong direction. These two sets of results correspond to the two couple geometries in which the end A was either gold-rich or silver-rich.

These differing results can be understood in terms of an impedance to free diffusion across the welded interface. Thus, if such an impedance existed, then, because the tracer was always applied to the end A, more tracer would remain on that side than if there were no impedance. A shift toward end A has a plus sign in Table II and it is seen that the shifts with a plus sign are larger than the shifts with a minus sign. (Notice the shift for couple No. 4 should have a minus sign, but it has been influenced toward end A so much that it has the wrong sign.) Couples Nos. 5 and 6, in which there was no chemical gradient, confirm the existence of this impedance by exhibiting a substantial shift in the plus direction. Similarly, for these couples it was found that after the diffusion anneal the ratio of total tracer in end A to that in B was about 1.02.

The results from couples Nos. 5 and 6 cannot be taken as an exact measure of the impedance for either couples Nos. 1 to 4 or couples Nos. 7 to 10, since neither diffusion times nor end compositions were reproduced. Using these results for an estimate, however, the difference between the two sets of results for couples Nos. 1 to 4 should then be roughly twice the shift in couples Nos. 5 and 6. For couples Nos. 7 to 10, the difference between the two sets should be somewhat smaller, since there was a general improvement in the quality of the welds beginning with couple No. 7. The experimental results certainly support these ideas.

In view of the existence of a diffusion impedance, the measured shifts should be either larger than or smaller than the predicted value, depending on whether the tracer was plated on the silver-rich or the gold-rich end. Thus the average value of $\bar{x}_{\text{expt}}$ for these two configurations should eliminate the impedance effect and is to be used when comparing experiment with theory. The results of this averaging are shown in Table III.[21] The theoretical values shown in Table III are also averages

TABLE III. Mean atom drifts averaged over tracer configurations.

Tracer	Approximate end compositions	$\bar{x}_{\text{theor}}$	$\bar{x}_{\text{expt}}$	Shift direction
Au^{198}	14 and 56 at.% Au	$14\pm 2\ \mu$	$10\pm 4\ \mu$	Toward 14 at.% Au
Ag^{110}	30 and 66 at.% Au	$23\pm 2\ \mu$	$30\pm 4\ \mu$	Toward 66 at.% Au

[19] J. R. Manning, Phys. Rev. **116**, 819 (1959).
[20] A. D. LeClaire and A. B. Lidiard, Phil. Mag. **1**, 518 (1956).

[21] The value of $\bar{x}_{\text{expt}}$ for couple No. 4 has been excluded from the average. This was done because of the unusual value of $\bar{x}_{\text{expt}}$ which indicates a poor weld in this particular case. If this result were not excluded, the first entry for $\bar{x}_{\text{expt}}$ in Table III would be 8.5μ.

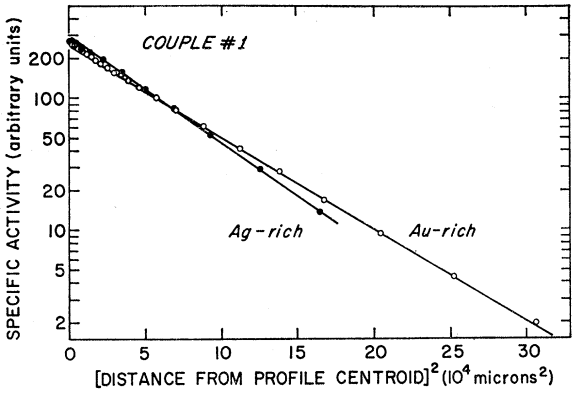

FIG. 8. Penetration plots of Au^{198} in couple No. 1. The origin is taken at the center of gravity of the Au^{198} distribution.

of the calculations, since these values contain c_i^*, which is affected by both the impedance and experimental error. The error limits on $\bar{x}_{\text{expt}}$ shown in Table III refer to the measurement, as mentioned earlier, and do not include impedance uncertainties. The agreement between theory and experiment is good for the gold tracer (approximately 24-h diffusion anneal), while for the silver tracer (approximately $5\frac{1}{2}$-h diffusion anneal) the experimental value is slightly high, but still almost within the estimated errors.

VI. OTHER MEASURABLE QUANTITIES

A. Voids

The existence of voids is suggested by the appearance of the Hf^{181} activity profile for couples Nos. 1 to 4. In these graphs there is a secondary peak of Hf^{181} activity on the silver-rich side of the main peak. It is suggested that voids, or pores, are formed near the original interface and that they subsequently move (due to the Kirkendall effect) to the silver-rich side, carrying some of the $Hf^{181}O_2$ particles with them. This anomalous Hf^{181} distribution is not noticed on couples Nos. 5 and 6, where there was no Kirkendall effect, nor on couples Nos. 7 to 10, where the Kirkendall shift was so small that the anomalous activity would be masked by the marker peak. Further evidence of voids was the appearance, during sectioning, of pitted surfaces and broken chips near the interface on its silver-rich side.

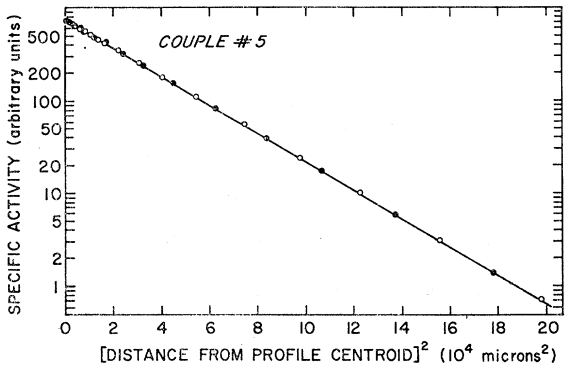

FIG. 9. Penetration plots of Au^{198} in couple No. 5. The origin is taken at the center of gravity of the Au^{198} distribution.

The existence of voids was confirmed by microscopic examination of two supplementary couples, similar to Nos. 1 to 4, which were not sectioned in the lathe, but were cut along a plane parallel to the diffusion direction. Examination revealed roughly spherical voids, approximately 15 μ in diameter, lying along a line about 62 μ to the silver-rich side of the "ghost line," which is assumed to be the interface position. This location of the voids agrees with the other observations discussed above.

Because of the short-circuiting effect of voids, their presence is not expected to interfere appreciably with the experiment. However, they do affect the lattice distortion term, but this effect was estimated to cause less than half a micron change in $\bar{x}$.

B. Tracer Diffusion Coefficients

Tracer diffusion coefficients $D^{*\prime}$ were measured from plots of logarithm of specific activity versus x^2. These values are listed in Table IV. For these plots $x=0$ was taken at the center of gravity of the tracer distribution so that two values of $D^{*\prime}$ were obtained for each couple. Three typical graphs are shown in Figs. 8–10. It should be pointed out that, due to the large density of data points, it was not possible in these figures to show distinctly all points near $x=0$.

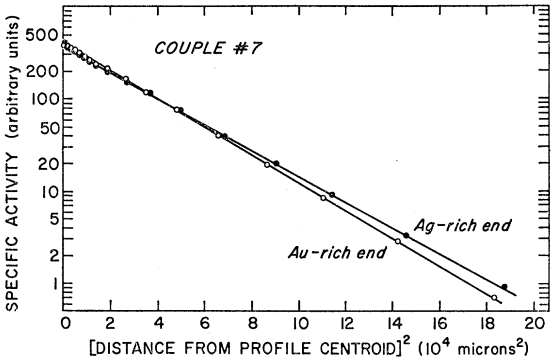

FIG. 10. Penetration plots of Ag^{110} in couple No. 7. The origin is taken at the center of gravity of the Ag^{110} distribution.

Except for couples Nos. 5 and 6, which were chemically homogeneous, the coefficients $D^{*\prime}$ do not represent self-diffusion coefficients because of the effect of the concentration gradient. These effects are, of course, the result of the same factors that influence the mean atom drift. Differences in the slopes of the two branches of the plots in Figs. 8–10 represent distortion from a symmetric Gaussian tracer distribution and are therefore due to diffusion forces which are nonuniform or nonsymmetric with respect to the center of the profile. Any uniform diffusion force would merely shift

TABLE IV. Tracer diffusion coefficient.

Couple	$D_{Au}^{*\prime}$ for ~14 at.% Au end	$D_{Au}^{*\prime}$ for ~56 at.% Au end	$D_{Au}^{*\prime}$ (max)	D_{Au}^{*}(min)
1	1.60×10^{-9} cm²/sec	1.86×10^{-9} cm²/sec		
2	1.61	1.86	1.76×10^{-9} cm²/sec	1.60×10^{-9} cm²/sec
3	1.68	1.89		
4	1.61	1.82		

Couple	$D_{Au}^{*\prime}$ for both ends	D_{Au}^{*}
5	1.66×10^{-9} cm²/sec	
6	1.64	1.60×10^{-9} cm²/sec

Couple	$D_{Au}^{*\prime}$ for ~30 a/0-Au end	$D^{*\prime}$ for ~66 at.% Au end	D_{Ag}^{*}(max)	D_{Ag}^{*}(min)
7	3.97×10^{-9} cm²/sec	3.65×10^{-9} cm²/sec		
8	4.04	3.65	3.90×10^{-9} cm²/sec	3.75×10^{-9} cm²/sec
9	4.04	3.73		
10	4.04	3.66		

the profile and this has been accounted for by measuring the distance x from the center of the profile.

The values of $D^{*\prime}$ for each group show good internal agreement and the averages of the $D^{*\prime}$ values for both branches are bracketed by the maximum and minimum values of the self-diffusion coefficients D^* over the composition range of each couple. These maximum and minimum D* values are shown in the last column of Table IV for the appropriate composition ranges. The values measured for couples Nos. 5 and 6, which should give ordinary self-diffusion coefficients, agree well with the published value of 1.60×10^{-9} cm²/sec.

C. Kirkendall Marker Shift and Interdiffusion Coefficient

Although these quantities could not be measured with high accuracy in the present work, they were nevertheless determined as an additional check on the reliability of the experiment. Values of x_m were measured on couples Nos. 1 to 4 and the two supplementary couples used in the microscopic examination. The measured x_m values were somewhat higher than the predicted values. Values of $\tilde{D}$ were measured in couples Nos. 1 to 4 and 7 to 10, the experimental results from couples Nos. 1 to 4 agreeing with theoretical prediction, while those from couples Nos. 7 to 10 being somewhat larger than predicted. These discrepancies may possibly be within experimental uncertainties.

VII. CONCLUSIONS

Because of the repeated measurements for a given physical situation and careful investigation into the experimental procedure itself, this experiment has yielded meaningful results on the effects of the activity coefficient and of the vacancy flow on diffusion in a concentration gradient. Reasonably good agreement has been found between experiment and theory, indicating that both have probably been handled properly.

The appearance in couples with short diffusion times of slightly higher values than predicted of the mean atom drift and the simultaneous indication of larger interdiffusion coefficients than predicted may have been caused by nonequilibrium vacancy concentrations resulting from large chemical gradients. Fara and Balluffi[22] have suggested that the product $\tilde{D}\tau$ must be smaller than about 10^{-5} cm² for these nonequilibrium effects to be appreciable. For the short-time experiments described here, $\tilde{D}\tau=8.5\times10^{-5}$ cm². Because of the sensitivity of this experiment, it is just possible that effects of nonequilibrium vacancy concentrations were apparent.

It is interesting that the lattice-distortion term was always larger than the vacancy-flow effect. Examination of the equations for $\bar{x}_{\text{vac flo}}$ and $\bar{x}_{\text{latt dist}}$ reveals a striking similarity. Since these two effects both result from the same net vacancy flow, it will generally be true that the lattice-distortion term will be important when the vacancy-flow term is important.

A substantial impedance to diffusion across the welded couple interface has been found to exist. Such an impedance has not been generally expected. The impedance presumably affects, not only the flow of tracer atoms, but also all other diffusion. It will therefore reduce the Kirkendall flow and cause experimental values of $\bar{x}$ to be smaller than predicted, at least for short diffusion times. This effect is expected to be small—it was about 2% in the present experiments—but an estimate of it must be made in any detailed comparison between theory and experiment.

Although good agreement between theory and experiment has been found for the mean atom drift, improvements in experimental accuracy can be made. By using larger specimens, diffusion times can be increased, thus increasing the magnitudes of the tracer shifts without increasing experimental uncertainties. The corresponding increase in $\tilde{D}\tau$ will also insure against the effect of nonequilibrium vacancy concentrations. A further increase in the vacancy-flow magnitude can be obtained by diffusing at temperatures lower than 950°C, where the ratio D_{Ag}^*/D_{Au}^* is larger.

The present work, nevertheless, by eliminating the influence of diffusion-coefficient gradients and by averaging out the perturbations of interface impedance, has shown that rather quantitative data can be obtained on the combined effect of vacancy flux and activity-coefficient gradient on the drift of tracer atoms. Although there may be a small discrepancy between theoretical expectations and experimental results which will be worth investigating further, on the whole, the agreement seems to be fairly reassuring.

[22] H. Fara and R. W. Balluffi, J. Appl. Phys. **30**, 325 (1959).